An analysis of the Brown-Biefeld effect

Reuven Ianconescu,* Daniela Sohar, and Moshe Mudrik

Shenkar College of Engineering and Design

When a voltage higher than 20 kv is applied on an asymmetric capacitor, the capacitor experiences a net force acting toward its thinner electrode. This effect is called Brown-Biefeld (BB) effect, in honor of its discoverers Thomas Townsend Brown and Paul Alfred Biefeld. A lot of theories have been proposed to explain the BB effect, and many speculations can be found on the net suggesting the BB effect to be an antigravitation effect that works in vacuum too. Other sources say the BB effect warps the space. However, in the recent years, more an more researchers attribute the BB effect to a unicharge ion wind . This work calculates the levitation force due to the ion wind and also presents experimental results which confirm the theoretical results. Our calculations use local coordinates analysis, and have a very low computing cost.

Key words: brown-biefeld, lifters, electrostatics, corona, ion drift, Deutsch assumption
PACS: 41.20.Cv, 52.30.-q, 41.20.-q

1. INTRODUCTION

The Brown-Biefeld (BB) effect has been discovered in 1920 by Thomas Townsend Brown and Paul Alfred Biefeld during their experiments with Coolidge X-ray tube. They observed a thrust acting toward the thin electrode. Thomas Townsend Brown made an extensive research on this effect and wrote several patents[1–3].

There is a site dedicated to the BB effect[4] and a site dedicated to experiments of this effect[5], but very few theoretical works have been written on the subject.

Some of those tried to explain the effect by electro-gravitation[6–8] or thermodynamics[9].

However, in the recent years more and more sources[10–13] attribute the effect to corona ionic air propulsion. In[13] a lot of experiments are described, and the thrust force is described by approximate formulae based on ion propulsion, and in[11] a full calculation of the thrust, based on the jet of the corona ion wind is performed.

The calculations in[11] were very accurate, but seemed to require a substantial amount of computing power.

In this work we also calculate the force due to ionic air propulsion, but we adopt a different approach, based on the Deutsch assumption[14], which has been extensively used in the unipolar charge flow literature[15–17], but also criticized[18].

The Deutsch assumption states that the equipotential surfaces of the Laplacian problem are equipotential also for the Poissonian problem, only with different values of potential. Of course under this assumption, the electric field lines of the Laplacian and Poissonian problems are in the same direction at any location.

As we shall see, the calculations based on Deutsch assumption[14], within the Warburg region[19,20] result in formulae which fit very well the experiment.

In Section 2 we explain the operation principle and the configuration on which we worked. We also present the equations that have to be solved.

In Section 3 we present the basics of the Deutsch assumption, for which cases it is accurate and for which cases it is an approximation. Also, we show how a first order correction can be applied in the inaccurate region. A profound analysis on the subject is presented.

In Section 4 we solve the Laplacian problem and calculate the capacitance. Those results are new, because as far as we know this Laplacian configuration has not been solved yet. Also, this Laplacian solution is needed for the Poissonian problem when Deutsch assumption

is used.

In Section 5 we solve the Poissonian problem using Deutsch assumption and a first order correction, and display the calculated force and current.

In Section 6 we describe our experiment and show the obtained results.

In Section 7 we compare the measured and calculated results and express our calculated results by approximate formulae.

The work is ended with some concluding remarks.

2. THE OPERATION PRINCIPLE AND THE CONFIGURATION

The picture of the lifter on which we did our experiments appears in Figure 1. The lifter is based on a thin anode wire at high voltage, over a grounded flat cathode. It is to be mentioned that the flat electrode must be vertical otherwise no propulsion can occur.

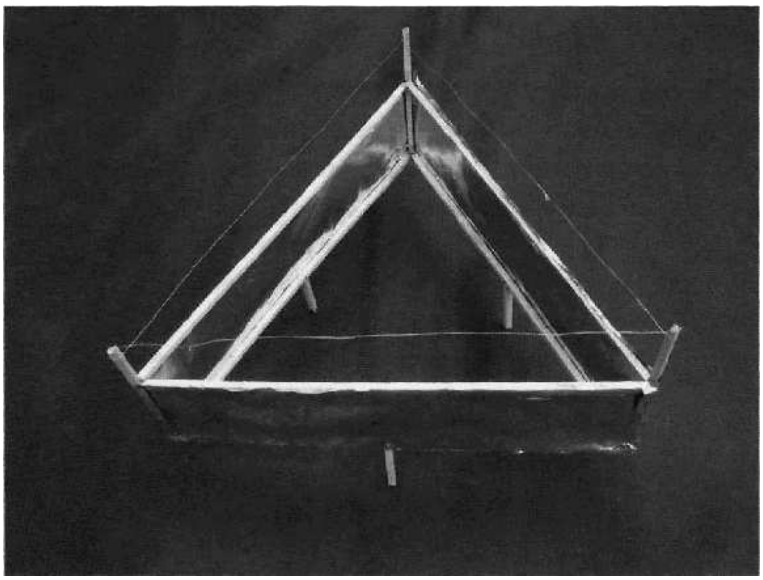

FIG. 1: The picture of the lifter we built.

The working principle is as follows: when a high enough voltage is supplied between anode and cathode, corona starts around the anode, and the positive ions are rejected from the anode. Those ions receive high velocities and ionize neutral air molecules, this way positive space charge is created in the air surrounding the electrodes. At bigger distances from the anode, the positive ions have less velocity, hence transfer momentum to neutral molecules,

without further ionizing them. The positive charge "feels" the force of the electric field and hence moves toward the cathode, according to the positive ion mobility coefficient, and the neutral molecules keep the inertia of the momentum they received. If the flat cathode were horizontal, not only ions but also the neutral molecules would hit the cathode and hence the forces on the anode and cathode would have been equal and opposite, hence no net thrust.

However, the cathode being vertical, and given the fact that the ions transfer *most* of their momentum to neutral molecules, those do not hit the cathode, but form an air jet downstairs, and by momentum conservation the lifter senses a net force upwards.

Hence, the thrust force is calculated as the total force on the space charge.

The shape must not necessarily be triangular, it may be rectangular or any other shape and, neglecting edge effects, the operation is described by a thin anode wire, over a vertical conducting plane. Hence we deal with a 2 dimensional problem described in Figure 2.

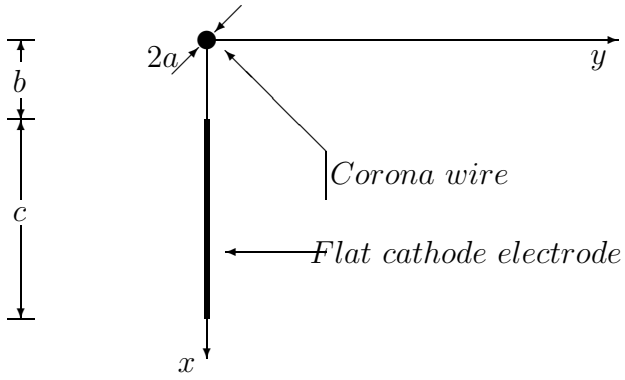

FIG. 2: The simplified 2D configuration. The corona wire is at coordinates $(0, 0)$ and its radius is a. The distance between the electrodes is called b, and the cathode length is c.

Our lifter has the following dimensions: $a = 0.075mm$, $b = 2.8cm$ and $c = 4cm$ (see Figure 2). Each side of the triangle is $0.2m$, hence if we calculate the thrust force per unit length, we have to multiply by the perimeter of $3 \times 0.2 = 0.6m$ to find the total force.

As long as the potential difference is below the corona inception voltage[21], there is no space charge, hence we have a *Laplacian* problem, defined by

$$\nabla^2 V_L = 0 \tag{1}$$

where the index "L" denotes the Laplacian solution. The boundary conditions are $V_L = V_0$ on the anode wire surface and $V_L = 0$ on the cathode wire surface, where V_0 is the applied

voltage. The electric field is $\bar{E_L} = -\bar{\nabla} V_L$.

In presence of space charge, different kinds of ions have different mobilities, defining the velocity of each ion as its mobility times the electric field. However, we use the average mobility[13,17,18] for positive air ions, known to be $\mu = 2 \times 10^{-4} m^2/v\ sec.$ Diffusion can usually be neglected[22], hence the unipolar nondiffusive drift of ions is described by

$$\bar{J} = \rho \bar{v} = \mu \rho \bar{E_P} \tag{2}$$

where ρ is the space charge per unit of volume and $\bar{E_P}$ is not the Laplacian field, but the *Poissonian* field, influenced by the space charge itself via:

$$\epsilon_0 \bar{\nabla} \cdot \bar{E_p} = \rho \tag{3}$$

Being a stationary problem, the current continuity condition $\bar{\nabla} \cdot \bar{J} = 0$ must hold. So the Poissonian problem may be formulated by: $\bar{\nabla} \cdot (\rho \bar{E_P}) = 0$ or

$$\bar{\nabla} \cdot (\nabla^2 V_P \ \bar{\nabla} V_P) = 0 \tag{4}$$

Clearly, this equation contains the 3rd derivative, hence one needs an additional boundary condition, and what is usually assumed is Kaptzov hypothesis[23].

Physically Kaptzov hypothesis means that once the potential difference has been raised sufficiently for the corona to start, the electric field near the corona conductor remains constant and equals the *inception* value, even when further raising the potential difference.

Felici[24] analyzed equation (4) and gave some particular solutions, and Feng[25] calculated an exact solution of (4) for concentric cylinders.

As mentioned before, equation (4) is easier to solve by using the Deutsch assumption[14]. It would be useful to understand the Deutsch assumption, for which cases it is accurate and for which cases it is an approximation and to what extent.

This item is discussed in the following section.

3. ANALYSIS OF THE DEUTSCH ASSUMPTION

The Deutsch[14] assumption states that the equipotential surfaces of the Laplacian problem,

defined by (1) are equipotential also for the Poissonian problem, defined by (4), only with different values of potential. Of course, under this assumption, the electric field lines of the Laplacian and Poissonian problems are in the *same direction* at any location.

Let us first take the curl of $\bar{J}$ in (2)

$$\bar{\nabla} \times \bar{J} = \mu(\bar{\nabla}\rho \times \bar{E_P} + \rho\ \bar{\nabla} \times \bar{E_P}) = \mu\bar{\nabla}\rho \times \bar{E_P} \tag{5}$$

because being a static problem, $\bar{\nabla} \times \bar{E_P} = 0$.

Now, we see that the condition for $\bar{\nabla} \times \bar{J} = 0$ is that $\bar{\nabla}\rho$ be *parallel* to $\bar{E_P}$, i.e.

$$\bar{\nabla}\rho \times \bar{E_P} = 0 \tag{6}$$

Let us suppose that we have a problem for which condition (6) is true. We know that always $\bar{\nabla} \cdot \bar{J} = 0$, so we see that $\bar{J}$ has zero curl, zero divergence and its tangential component near the conductors is zero.

But those are exactly the conditions satisfied by $\bar{E_L}$! Those conditions set the function $\bar{E_L}$ up to a multiplying constant, established by the potential difference.

Exactly the same way, the above conditions set the function $\bar{J}$ up to a multiplying constant, established by the total current.

Hence, if (6) is satisfied, $\bar{E_L}$ and $\bar{J}$ are the *same functions*, up to a multiplying constant K so that one may use:

$$\bar{J} = K\bar{E_L} \tag{7}$$

Now, clearly, if (6) is true, Deutsch assumption becomes *a fact* instead of an *assumption.* This can be shown in the following way: for Deutsch assumption to hold true, $\bar{E_L}$ and $\bar{E_P}$ must be in the *same direction* at any location. Hence $\bar{E_P} = f\bar{E_L}$, where f is a *scalar function.* But f cannot be any function, because the curl of $\bar{E_P}$ must be 0. Hence,

$0 = \bar{\nabla} \times \bar{E_P} = \bar{\nabla} \times (f\bar{E_L}) = \bar{\nabla}f \times \bar{E_L} + f\ \bar{\nabla} \times \bar{E_L} = \bar{\nabla}f \times \bar{E_L}$

So the multiplying function f must have its gradient parallel to $\bar{E_L}$. But from equations (7) and (2), we see that

$$\bar{E_P} = K\frac{1}{\mu\rho}\bar{E_L} \tag{8}$$

and from (6) $\bar{\nabla}\frac{1}{\rho}$, like $\bar{\nabla}\rho$ is parallel to $\bar{E_L}$ and to $\bar{E_P}$.

The question is now in which cases the Deutsch assumption becomes a fact?

Let us first look at some simple and well known configurations: between parallel plates, clearly with or without space charge the equipotential surfaces are parallel to the plates. The same is true for concentric cylinders or concentric spheres: with or without space charge the equipotential surfaces are concentric cylinders or spheres, respectively. The common physical characteristic for all those cases is that the electric field lines are *straight*.

Now we prove that Deutsch assumption holds *exactly* if the field lines $\bar{E_L}$ are *straight*.

The proof is based on Figure 3, which describes Poissonian curved field lines in local coordinates (we omit here the "L" index). Requiring the curl of $\bar{E}$ to be 0 is equivalent to requiring $\oint \bar{E} \cdot \bar{dl} = 0$ along the closed curve in Figure 3. This results in $E_1 L_1 - E_2 L_2 = 0$. $L_1 \neq L_2$ if the field lines are curved, hence $E_1 \neq E_2$, or in other words, the electric field *must* depend on the coordinate v (see Figure 3). In such case, ρ, which is proportional to the divergence of $\bar{E}$ depends on v, and hence its gradient has a component perpendicular to $\bar{E}$.

On the other hand, if the field lines are straight, $L_1 = L_2$, hence $E_1 = E_2$, so $\bar{E}$ does not depend on v, and therefore the gradient of ρ is parallel to $\bar{E}$, and this completes the proof.

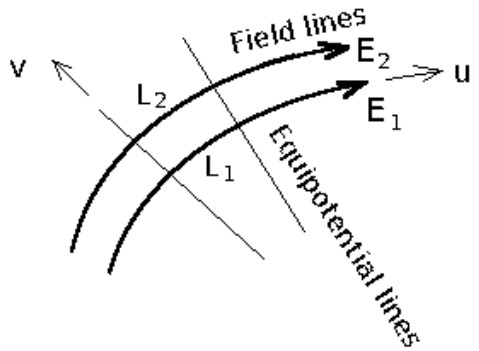

FIG. 3: Curved electric field lines in local coordinates. The coordinate u is in the local direction of the field, and the orthogonal coordinate v is in the local direction of the equipotential line.

The conclusion from this analysis is that as straighter the field lines are, the usage of Deutsch assumption results in more and more accurate results. To put this in another way,

the Poissonian result will be more accurate in the regions where the Laplacian field lines are straight.

Now we want to see the implications of formulating the solution with the Deutsch assumption, in the regions where the Laplacian field lines are not "straight enough". In such region, because we "obliged" the curl of J to be 0, we get from (7) and (5):

$$\bar{\nabla} \times \bar{E_P} = \frac{-1}{\rho} \bar{\nabla}\rho \times \bar{E_P} \neq 0 \tag{9}$$

because condition (6) is not true in those regions. This implies that outside the correctness region, the E_p field lines will sum to inaccurate values. The solution becomes less accurate, as we get farther from the straight lines field region.

This inaccuracy may be compensated with a first order correction, by letting the constant K in (7) be a function in the region where a correction is needed. To keep $\bar{\nabla} \cdot \bar{J} = 0$, one can easily see that K can only be a function of v (see Figure 3). Such a first order correction is implemented in Sect. 5, where we solve the Poissonian problem.

So, for using Deutsch assumption in the Poissonian problem, we need the solution to the Laplacian problem first, and this is done in the next section.

4. SOLUTION OF THE LAPLACIAN PROBLEM

There are many ways to solve the Laplacian problem (analytic or numeric) and we chose to solve it analytically, by separation of variables in cylindrical coordinates.

The schematic configuration in Figure 2, does not allow to properly define boundary conditions in separate variables in cylindrical coordinates, hence we will make a slight change to this configuration.

Anyhow the configuration in Figure 2 is not accurate, because it does not show the width of the flat cathode. In practice the cathode must have a finite width, and more than that, the curvature radius of the cathode at the location $(x = b, y = 0)$ (see Figure 2) must be big enough so that *no corona* can be formed there[21].

The modified configuration is described in Figure 4.

The flat cathode surface is now defined along $\varphi = \pm\alpha$, where α is a fixed small angle of about 1.3^o (based on the thickness of the cathode in our lifter). The cathode edge at

$(x = b, y = 0)$ has now a big radius of curvature b and in addition is *concave*, hence does not develop corona. And at last, we take the cathode length c to infinity: the main interaction is between the electrodes and using a finite length c would be still solvable analytically, but would be an unnecessary complication.

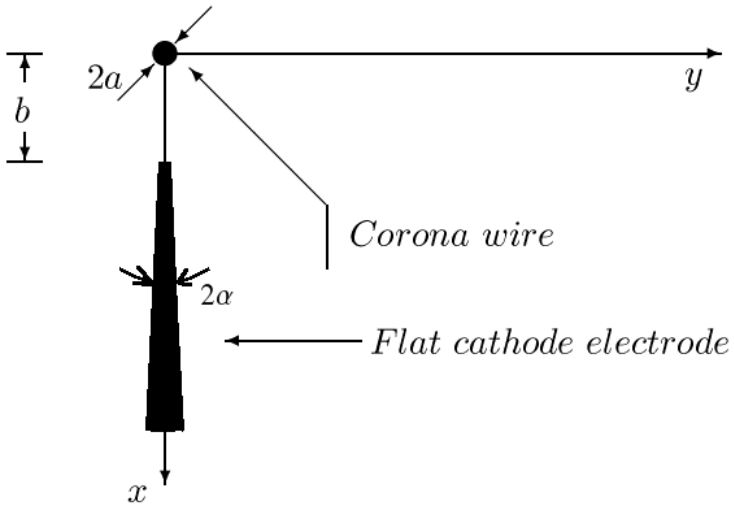

FIG. 4: Configuration adapted to cylindrical coordinates. The cathode contour is described by the lines $r = b$, and $\varphi = \pm\alpha$.

We define the potential V_1 for the region $a \leq r \leq b$ and $0 \leq \varphi \leq 2\pi$ and the potential V_2 for the region $r \geq b$ and $\alpha \leq \varphi \leq 2\pi - \alpha$. The boundary conditions are:

$$V_1(r = a, \varphi) = V_0 \tag{10}$$

where V_0 is the applied voltage.

Because of the mirror symmetry around the x axis, we require

$$V_1(r, \varphi) = V_1(r, 2\pi - \varphi) \ . \tag{11}$$

The potential continuity at $r = b$ gives

$$V_1(r = b, \varphi) = \begin{cases} 0 & 0 \leq \varphi \leq \alpha \\ 0 & 2\pi - \alpha \leq \varphi \leq 2\pi \\ V_2(r = b, \varphi) & \alpha \leq \varphi \leq 2\pi - \alpha \end{cases} \tag{12}$$

and the normal field continuity at $r = b$ requires

$$\partial_r V_1(r=b, \alpha \leq \varphi \leq 2\pi - \alpha) = \partial_r V_2(r=b, \alpha \leq \varphi \leq 2\pi - \alpha) \ . \tag{13}$$

The potential is 0 on the sides of the big conductor

$$V_2(r, \varphi = \alpha) = V_2(r, \varphi = 2\pi - \alpha) = 0 \tag{14}$$

and must go to 0 at $r \to \infty$

$$V_2(r \to \infty, \alpha \leq \varphi \leq 2\pi - \alpha) = 0 \tag{15}$$

We will use the well know solutions for the Laplace equation in cylindrical coordinates, for the z independent case, given by the trivial solution $D - E \ln r$ (where D and E are constants) plus the non trivial solution:

$$\sum_\nu (A_\nu r^\nu + B_\nu r^{-\nu})(C_\nu \cos(\nu\varphi) + D_\nu \sin(\nu\varphi)) \tag{16}$$

where one may consider only non negative values of ν, because negative ν just switches the roles of A_ν and B_ν.

Let us start with V_2. Condition (15) excludes the trivial solution and the r^ν solution which diverge at $r \to \infty$. Also, the requirement $V_2(r, \varphi = \alpha) = 0$ in (14) imposes a combination between the sin and cos terms in (16) of the form $\sin(\nu(\varphi - \alpha))$ and the constant B_ν may be normalized for convenience to $B_\nu / b^{-\nu}$. Hence we may write the following expression for V_2:

$$V_2 = \sum_\nu B_\nu (r/b)^{-\nu} \sin(\nu(\varphi - \alpha)) \tag{17}$$

To satisfy the requirement $V_2(r, \varphi = 2\pi - \alpha) = 0$ in (14), we need $\sin(\nu(2\pi - \alpha - \alpha)) = 0$, or $\nu(2\pi - 2\alpha) = m\pi$ (where m is a positive integer), thus giving the values of $\nu = \frac{m}{2}\frac{1}{1-\alpha/\pi}$. So the expression for V_2 may be written as:

$$V_2 = \sum_{m=1}^{\infty} B_m (r/b)^{-\frac{m}{2}\frac{1}{1-\alpha/\pi}} \sin\left(\frac{m}{2}\frac{\varphi - \alpha}{1 - \alpha/\pi}\right) \tag{18}$$

Now we look for an expression for V_1. Because the non trivial solution is φ dependent for

any r, to satisfy condition (10), we need also the trivial solution. Also, because V_1 is defined in a region with circular continuity, adding 2π to φ must result in the same potential, hence ν must be an integer, say m. For satisfying (11) only the cos solution must be taken, and again, we may normalize the constants so that the power is on r/a instead of r, so we may write the following expression for V_1:

$$V_1 = D - E\ln r + \sum_{m=0}^{\infty} \left(A_m (r/a)^m + C_m (r/a)^{-m}\right) \cos(m\varphi) \tag{19}$$

To satisfy condition (10), the $m \neq 0$ terms of the non trivial part of (19), must be identically 0 for $r = a$. Given that the functions $\cos(m\varphi)$ are orthogonal in the interval $0 \leq \varphi \leq 2\pi$, each term of the series must vanish for $r = a$, hence we get $A_m = -C_m$, for $m \neq 0$. The $m = 0$ term gives just a constant, which may be absorbed in the trivial solution, but it proves convenient to name the $m = 0$ term L_0, and to scale separately the trivial solution so that it results in an arbitrary constant V' for $r = a$, and 0 for $r = b$, so that $D - E\ln r = V'\left(1 - \frac{\ln(r/a)}{\ln(b/a)}\right)$. So we may write the following expression for V_1:

$$V_1 = V'\left(1 - \frac{\ln(r/a)}{\ln(b/a)}\right) + L_0 + \sum_{m=1}^{\infty} A_m \left((r/a)^m - (r/a)^{-m}\right) \cos(m\varphi) \tag{20}$$

It is to be mentioned that we do not lose any generality with the above scaling of the trivial solution, because after scaling, the trivial solution plus L_0 result in $V' + L_0$ for $r = a$ and L_0 for $r = b$, and the relationship between these two values has not been established yet.

The reason for choosing this approach is that all the unknowns, namely A_m and L_0 in (20) and B_m in (18) must be proportional to the applied voltage V_0, so we may calculate them with the aid of an arbitrary V', and obtain $V_1(r = a, \varphi) = V' + L_0$, which can be scaled eventually by a factor $V_0/(V' + L_0)$ to be equal to V_0. So we may set from now on $V' \equiv 1$, and remember to multiply everything by $V_0/(1 + L_0)$.

One may verify that the alternative approach of absorbing L_0 in the trivial solutions results in much more complicated equations.

We require condition (13):

$$\frac{-1}{\ln(b/a)} + \sum_{m=1}^{\infty} mA_m \left((b/a)^m + (b/a)^{-m}\right)\cos(m\varphi) = \sum_{m=1}^{\infty} \frac{-mB_m}{2(1-\alpha/\pi)} \sin\left(\frac{m}{2}\frac{\varphi-\alpha}{1-\alpha/\pi}\right) \quad (21)$$

and the above condition holds for $\alpha \le \varphi \le 2\pi - \alpha$. In this range, the $\sin\left(\frac{m}{2}\frac{\varphi-\alpha}{1-\alpha/\pi}\right)$ functions are orthogonal, so we multiply (21) by $\sin\left(\frac{n}{2}\frac{\varphi-\alpha}{1-\alpha/\pi}\right)$ (for any positive integer n) and integrate on φ over the range $[\alpha, 2\pi-\alpha]$. We use the following integrals:

$$\int_{\alpha}^{2\pi-\alpha} \sin\left(\frac{n}{2}\frac{\varphi-\alpha}{1-\alpha/\pi}\right) d\varphi = \begin{cases} 0 & n \text{ odd} \\ \frac{4}{n}(1-\alpha/\pi) & n \text{ even} \end{cases} \quad (22)$$

$$\int_{\alpha}^{2\pi-\alpha} \sin\left(\frac{n}{2}\frac{\varphi-\alpha}{1-\alpha/\pi}\right) \sin\left(\frac{m}{2}\frac{\varphi-\alpha}{1-\alpha/\pi}\right) d\varphi = \pi(1-\alpha/\pi)\delta_{mn} \quad (23)$$

where δ_{mn} is the Kronecker delta, and:

$$\int_{\alpha}^{2\pi-\alpha} \sin\left(\frac{n}{2}\frac{\varphi-\alpha}{1-\alpha/\pi}\right) \cos(m\varphi) d\varphi = G_{nm} \quad (24)$$

where G_{nm} is a matrix defined by:

$$G_{nm} = \begin{cases} 0 & & n \text{ odd} \\ \cos(m\alpha)\frac{n/(1-\alpha/\pi)}{((n/2)/(1-\alpha/\pi))^2 - m^2} & m \ne (n/2)/(1-\alpha/\pi) & n \text{ even} \\ -(\pi-\alpha)\sin(m\alpha) & m = (n/2)/(1-\alpha/\pi) & n \text{ even} \end{cases} \quad (25)$$

The last case defined by $m = (n/2)(1-\alpha/\pi)$ is not likely to happen if $\alpha \to 0$, except for very specific values of α, but we calculated this case for completeness. It is to be mentioned that for this case $\alpha/\pi = 1 - n/(2m)$, for some specific m and n, hence $m\alpha = m\pi - n\pi/2$ is equivalent to the points $\pi/2$ or $3\pi/2$ on the unity circle, so that $\cos m\alpha = 0$, and this has been used in the above calculation. Also, $\sin(m\alpha)$ could be written as $(-1)^{m-n/2-1/2}$.

After performing the above integrals, we obtain from (21) the following result for the B coefficients in (18):

$$-\frac{1}{2}\pi n B_n = \begin{cases} 0 & n \text{ even} \\ -\frac{4}{n}(1-\alpha/\pi)\frac{1}{\ln(b/a)} + \sum_{m=1}^{\infty} G_{nm} mA_m \left((b/a)^m + (b/a)^{-m}\right) & n \text{ odd} \end{cases} \quad (26)$$

This result implies that B_n are 0 for even n, and this is expected because of the mirror symmetry around the x axis.

Now we require conditions (12):

$$L_0+\sum_{m=1}^{\infty} A_m\left((b/a)^m-(b/a)^{-m}\right)\cos(m\varphi)=\begin{cases} 0 & 0\le\varphi\le\alpha \\ 0 & 2\pi-\alpha\le\varphi\le 2\pi \\ \sum_{m=1}^{\infty} B_m \sin\left(\frac{m}{2}\frac{\varphi-\alpha}{1-\alpha/\pi}\right) & \alpha\le\varphi\le 2\pi-\alpha \end{cases} \tag{27}$$

The above condition is defined for $0 \le \varphi \le 2\pi$. In this range, the $\cos(m\varphi)$ functions are orthogonal, so we multiply (27) by $\cos(n\varphi)$ and integrate on φ over the range $[0, 2\pi]$, for n being any non negative integer.

First, if we do it for $n = 0$, the sum on the left side vanishes, and using (22), with m instead of n, we obtain the following expression for L_0:

$$L_0 = \frac{2}{\pi}(1-\alpha/\pi)\sum_{m=1\ (\text{odd})}^{\infty}\frac{B_m}{m} \tag{28}$$

and we could have even omitted the word "odd", because we already know that the even B coefficients from (18) are 0.

Now we multiply (27) by $\cos(n\varphi)$ and integrate from $\varphi = 0$ to 2π, for $n \neq 0$. This time L_0 vanishes, and after using:

$$\int_0^{2\pi}\cos(n\varphi)\cos(m\varphi)d\varphi = \pi\delta_{mn} \tag{29}$$

where δ_{mn} is the Kronecker delta, and the result (24) for m and n switched, we obtain from (27) the following result for the A coefficients in (20):

$$\pi A_n\left((b/a)^n-(b/a)^{-n}\right) = \sum_{m=1\ (\text{odd})}^{\infty} G_{mn}B_m \tag{30}$$

again we could have omitted the word "odd" because the coefficients B_m and G_{mn} are 0 for even m.

Knowing that the even coefficients B are 0, we set in (18) $m = 2l-1$, but for simplicity we will call B_{2l-1} just B_l, in other words we redefine the B coefficients to include only the odd ones. So we rewrite V_2 as:

$$V_2 = \sum_{l=1}^{\infty} B_l (r/b)^{-\frac{l-1/2}{1-\alpha/\pi}} \sin\left((l-1/2)\frac{\varphi-\alpha}{1-\alpha/\pi}\right) \tag{31}$$

In the same way, eq. (28) may be rewritten as:

$$L_0 = \frac{2}{\pi}(1-\alpha/\pi)\sum_{l=1}^{\infty}\frac{B_l}{2l-1} \tag{32}$$

and eq. (26) and (30) may be rewritten as:

$$-\frac{1}{2}\pi(2l-1)B_l = -\frac{4}{2l-1}(1-\alpha/\pi)\frac{1}{\ln(b/a)} + \sum_{m=1}^{\infty} G_{lm} m A_m \left((b/a)^m + (b/a)^{-m}\right) \tag{33}$$

and

$$\pi A_n \left((b/a)^n - (b/a)^{-n}\right) = \sum_{l=1}^{\infty} G_{ln} B_l \tag{34}$$

where the matrix G_{nm} has been redefined accordingly, by setting $n = 2l-1$:

$$G_{lm} = \begin{cases} \cos(m\alpha)\frac{(2l-1)/(1-\alpha/\pi)}{((l-1/2)/(1-\alpha/\pi))^2 - m^2} & m \neq (l-1/2)/(1-\alpha/\pi) \\ -(\pi-\alpha)\sin(m\alpha) & m = (l-1/2)/(1-\alpha/\pi) \end{cases} \tag{35}$$

or, as mentioned after (25), for the case $m = (l-1/2)/(1-\alpha/\pi)$, one may replace $\sin(m\alpha)$ by $(-1)^{m-l}$.

Now we will rewrite eq. (33) and (34) in matrix form, to solve 2 matrix equations with 2 unknown vectors for the coefficients A and B, then find L_0 with (32) and eventually calculate the potential and scale it by the factor $V_0/(1+L_0)$.

To rewrite eq. (34) in matrix form we define the diagonal matrix $\mathcal{Q}$, by its components as $Q_{mn} \equiv \left((b/a)^m - (b/a)^{-m}\right)\delta_{mn}$, and obtain:

$$\pi \mathcal{Q}\overline{A} = \mathcal{G}^T \overline{B} \tag{36}$$

To rewrite eq. (33) in matrix form we define the diagonal matrices $\mathcal{P}$, by $P_{mn} \equiv \left((b/a)^m + (b/a)^{-m}\right)\delta_{mn}$, $\mathcal{S}$, by $S_{mn} \equiv (2m-1)\delta_{mn}$ and $\mathcal{J}$, by $J_{mn} \equiv m\delta_{mn}$. We also

define the column vector $\overline{K}$ by its components $K_m = 1$, and obtain:

$$-\frac{1}{2}\pi\mathcal{S}\overline{B} = -4(1-\alpha/\pi)\frac{1}{\ln(b/a)}\mathcal{S}^{-1}\overline{K} + \mathcal{G}\mathcal{J}\mathcal{P}\overline{A} \tag{37}$$

We isolate $\overline{B}$ from (37):

$$\overline{B} = \frac{8}{\pi}(1-\alpha/\pi)\frac{1}{\ln(b/a)}\mathcal{S}^{-2}\overline{K} - \frac{2}{\pi}\mathcal{S}^{-1}\mathcal{G}\mathcal{J}\mathcal{P}\overline{A} \tag{38}$$

and set it in (36) to obtain a closed form solution for $\overline{A}$:

$$\overline{A} = \frac{8}{\pi}(1-\alpha/\pi)\frac{1}{\ln(b/a)}(\pi\mathcal{Q} + \frac{2}{\pi}\mathcal{G}^T\mathcal{S}^{-1}\mathcal{G}\mathcal{J}\mathcal{P})^{-1}\mathcal{G}^T\mathcal{S}^{-2}\overline{K} \tag{39}$$

Clearly, for $\alpha = \pi$ (concentric cylinders), $\overline{A}$, $\overline{B}$ and L_0 are all 0, hence $V_2 = 0$ and we are left only with the trivial solution for V_1, as expected.

This calculation has been carried out numerically. As smaller α we use, we need to keep bigger dimensions in the matrices, to obtain convergence. Figure 5 shows the potential in a 3D plot, for the physical values of our lifter, where V_0 is normalized to 1. The matrices and vectors have been cut to the dimension of 119. Because of the mirror symmetry around the x axis, we drew the potential only for positive y.

We derive now the electric field. For region 1 we obtain the radial field:

$$E_{1r} = -\frac{\partial V_1}{\partial r} = \frac{V_0}{1+L_0}\frac{1}{r}\left[\frac{1}{\ln(b/a)} - \sum_{m=1}^{\infty} mA_m\left((r/a)^m + (r/a)^{-m}\right)\cos(m\varphi)\right] \tag{40}$$

and the circular field:

$$E_{1\varphi} = -\frac{1}{r}\frac{\partial V_1}{\partial \varphi} = \frac{V_0}{1+L_0}\frac{1}{r}\sum_{m=1}^{\infty} mA_m\left((r/a)^m - (r/a)^{-m}\right)\sin(m\varphi) \tag{41}$$

For region 2 we obtain the radial field:

$$E_{2r} = -\frac{\partial V_2}{\partial r} = \frac{V_0}{1+L_0}\frac{1}{r}\sum_{l=1}^{\infty}\frac{l-1/2}{1-\alpha/\pi}B_l(r/b)^{-\frac{l-1/2}{1-\alpha/\pi}}\sin\left((l-1/2)\frac{\varphi-\alpha}{1-\alpha/\pi}\right) \tag{42}$$

and the circular field:

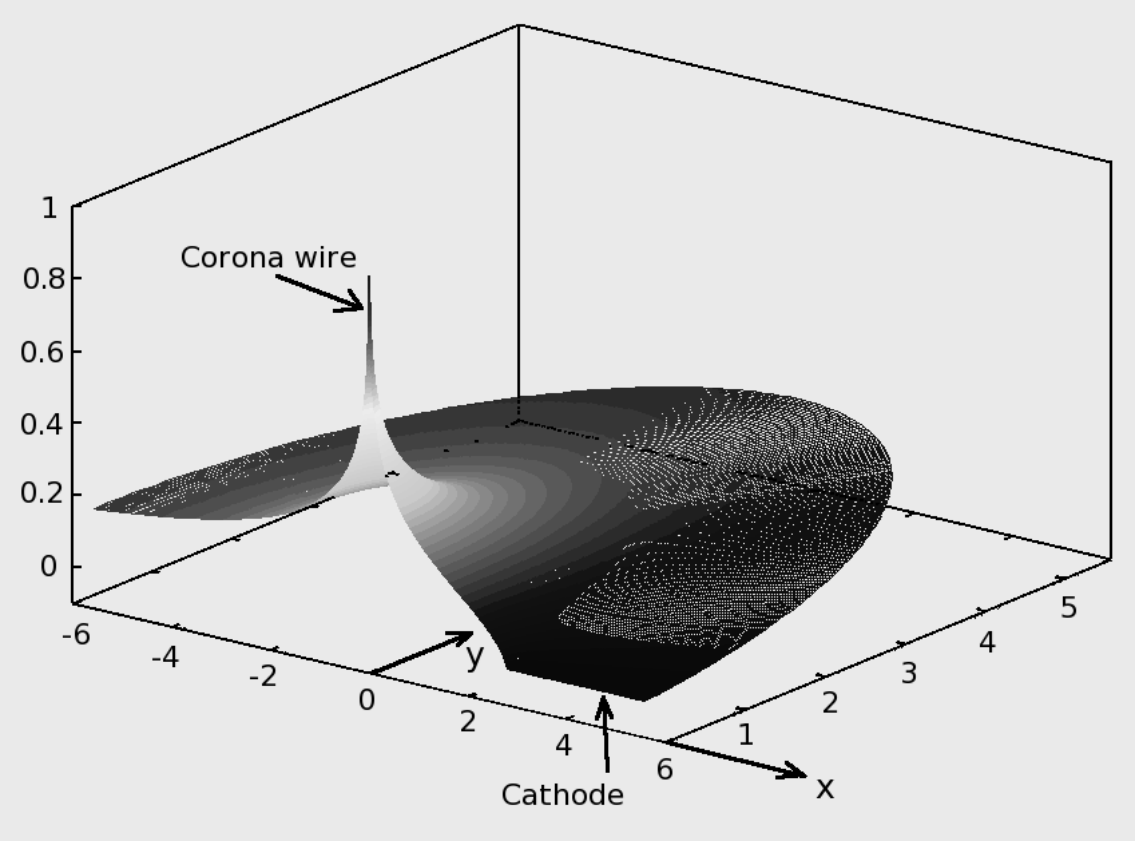

FIG. 5: 3D plot for the potential. V_0 is normalized to 1.

$$E_{2\varphi} = -\frac{1}{r}\frac{\partial V_2}{\partial \varphi} = -\frac{V_0}{1+L_0}\frac{1}{r}\sum_{l=1}^{\infty}\frac{l-1/2}{1-\alpha/\pi}B_l(r/b)^{-\frac{l-1/2}{1-\alpha/\pi}}\cos\left((l-1/2)\frac{\varphi-\alpha}{1-\alpha/\pi}\right) \tag{43}$$

It would be useful to calculate the capacitance. The charge per unit of surface on the anode is $\eta = \epsilon_0 E_{1r}(r=a,\varphi)$, and the charge per unit of length is given by $\lambda = \int_0^{2\pi} a\, d\varphi\, \eta$. Clearly, the integral on φ zeroes the sum in (40) and we are left with:

$$\lambda = \frac{2\pi\epsilon_0 V_0}{\ln(b/a)(1+L_0)} \tag{44}$$

So the capacitance per unit of length is:

$$C' = \frac{\lambda}{V_0} = \frac{2\pi\epsilon_0}{\ln(b/a)(1+L_0)} \tag{45}$$

Of course, for $\alpha = \pi$, $L_0 = 0$ (see (32)) and we recover the known formula for the

capacitance per unit of length for concentric cylinders.

We are of course interested in small α, so we calculated the values of L_0 for different ratios b/a, and fit an approximate formula for it - see Figure 6. It comes out that for $\alpha < \pi/100$, L_0 can be expressed as:

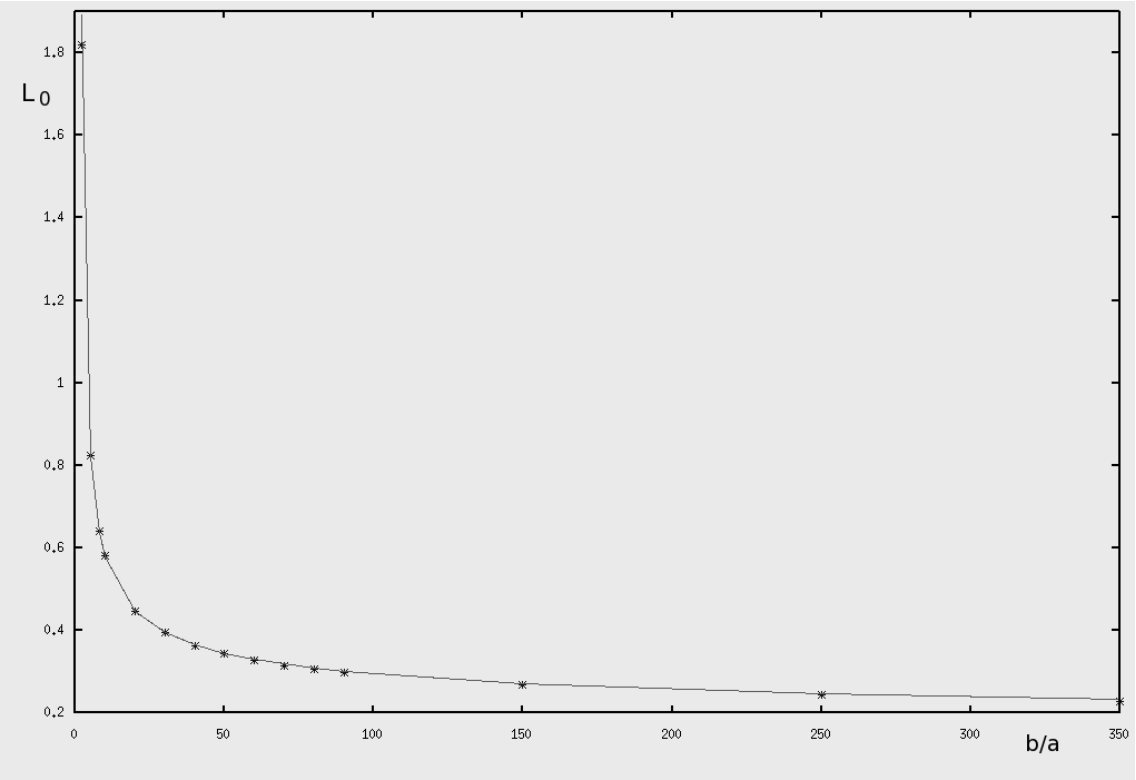

FIG. 6: Values of L_0 for $\alpha = 1.3^o$. The stars are the exact calculated values, and the continuous line represents the fitted curve values given by eq. 46. This fitted curve is valid for $\alpha < \pi/100$ rd $= 1.8^o$

$$L_0 \approx \frac{1.3035}{\ln(b/a)} + 0.011 \tag{46}$$

resulting in the following approximate formula for the capacitance per unit of length:

$$C' \approx \frac{2\pi\epsilon_0}{1.011\ \ln(b/a) + 1.3035} \tag{47}$$

If we set the values for our lifter: $a = 0.075mm$ and $b = 2.8cm$ into (47) we get $C' = 7.63pF/m$, and multiplying by the lifter's perimeter $0.6m$, the calculated capacitance comes out $C_{\text{calculated}} = 4.57pF$. To check the validity of this result we measured the capacitance of our lifter and got $C_{\text{measured}} = 4pF \pm 5\%$, which is quite close to the calculated result.

It is also useful to get a relation between the applied voltage V_0 and the field intensity on the anode. Of course, the field on the anode wire is not constant, and depends of φ. But for a thin anode ($b \gg a$), the field is almost constant (see also discussion in the next section).

One may verify that for $r = a$ the absolute value of the sum in (40) is much smaller than $\frac{1}{\ln(b/a)}$ hence we may write the approximate expression:

$$\frac{V_0}{E_{1r}(r=a,\varphi)} \approx (1+L_0)\; a\ln(b/a) \approx a(1.3035 + 1.011\ln(b/a)) \tag{48}$$

where the second expression is a further approximation which uses (46).

Again, for $\alpha = \pi$, $L_0 = 0$, and we recover the known expression of this relation for concentric cylinders.

In Figure 7 we show the equipotential surfaces and the field lines - those are needed in the next section. The Warburg[19,20] region can be seen also in Figure 7, and will be referred to in the next section.

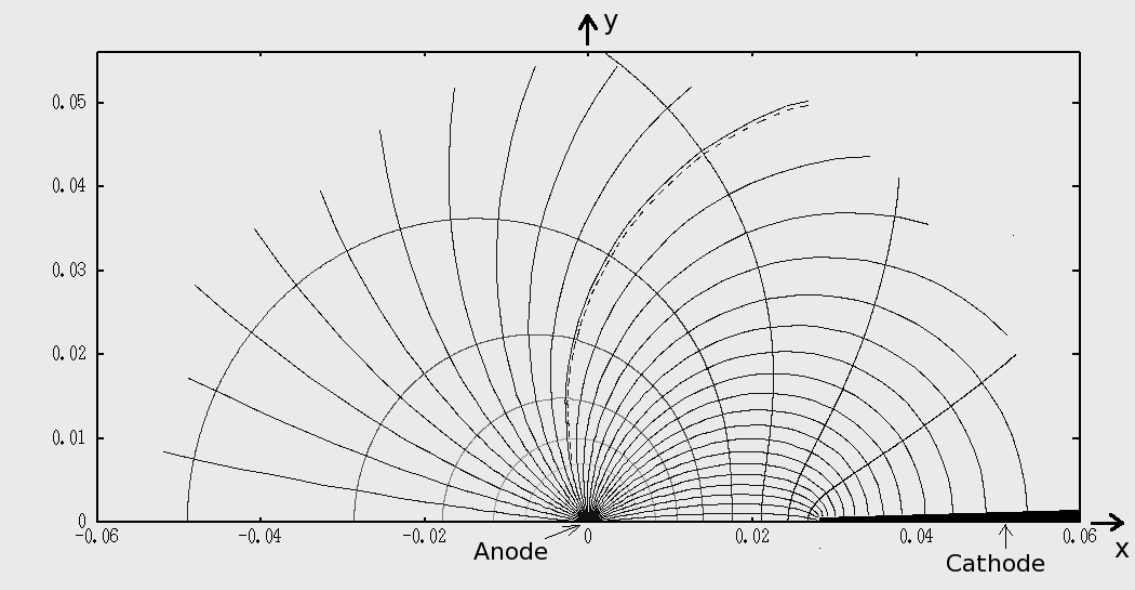

FIG. 7: The lines emerging from the anode are the electric field lines, and those perpendicular to them are the equipotential surfaces. The axes are in units of meter. The coordinates u and v denote the local direction of the field and the equipotential lines, respectively. The dashed line shows the electric field line which delimits the Warburg region. This field line passes through the point $(x = b, y = b/\tan(60^o))$. Only the $y > 0$ is shown, because of the mirror symmetry around the x axis

5. THE POISSONIAN PROBLEM

In this section we use the Laplacian results obtained in the previous section to solve the Poissonian problem, i.e. the state of the system when the applied voltage is bigger than the corona inception voltage.

F.W. Peek[21] made an extensive research on corona inception for different geometries like concentric cylinders, parallel wires, etc. and published the results in his book. For all the configurations involving corona around a thin wire of radius a, the electric field on the surface of the wire at which corona begins (at room temperature) is given by $E_i = 3 \times 10^6(1 + p/\sqrt{a})\ v/m$, where $p \approx 0.03\ \sqrt{m}$ with *very slight* variations of less than 2% for different geometries, with different asymmetries for the electric field.

We do not have the exact value for our geometry, but as explained by Peek himself, before corona starts, the field very close to a thin wire behaves like the field on the surface (which is almost constant if the wire is thin) times the wire radius, divided by the distance from the wire. So when having the above E_i value *on the wire surface*, one can easily find that at a distance of $p\sqrt{a}$ from the wire surface the field is $3 \times 10^6\ v/m$, this way assuring a field of more than $3 \times 10^6\ v/m$ in a wide enough region around the wire to allow corona to start.

So we can safely use Peek formula:

$$E_i = 3 \times 10^6(1 + 0.03/\sqrt{a})\ v/m \tag{49}$$

as has be done a lot in the literature, for different configurations of thin wire electrode near any other electrode[11,18,25].

Given $a = 0.075mm$, we know that for our case $E_i = 13.392\ Mv/m$.

Now we can find at which voltage the corona starts, i.e. the Corona Inception Voltage (CIV). The CIV is the voltage for which the Laplacian field on the surface of the corona wire equals to 13.392 Mv/m. For this we do not have to use Peek formula for CIV, we have the Laplacian solution for our problem. Using the approximation (48), results in 7.32 Kv or running the solution and measuring the exact relation results in 7.42 Kv, so the difference is less than 2%. Hence we may use:

$$\text{CIV} = 7.4\ Kv \tag{50}$$

Because of the asymmetry around the anode, the field on the corona surface is not completely uniform, and that is the reason for the slight variations in p in Peek formula for different asymmetric configurations. But fortunately, the corona wire being very thin, the field on the corona wire surface is almost uniform (up to variations of 0.5%), so we do not have to worry about it. (See also discussion before (48)).

So for a voltage bigger than the CIV, the Laplacian solution is not valid anymore, and we need the solution to the Poissonian problem.

This requires the simultaneous solution of (3)) and (2)), where for J we use (7).

The coefficient K in (7) is unknown, but given the fact that our solution is accurate for $y = 0$, i.e. where the field lines are straight (see discussion in Sect. 3), one can iterate the coefficient K in this region to get $\int_a^b E\,\mathrm{d}x = V_0$, where V_0 is the potential difference for which we solve.

The numerical solution is described in Figure 8, which is a zoom on a region of Figure 7.

The "P" prefix for Poissonian is omitted, for brevity.

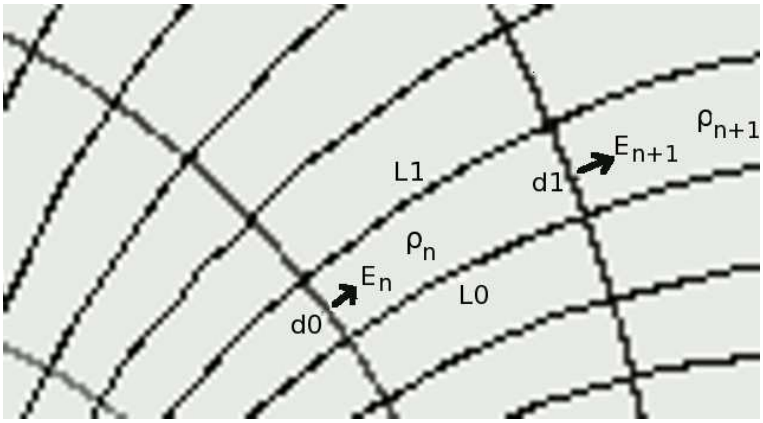

FIG. 8: The calculations are done along the Laplacian field lines, and start with $n = 0$ on the anode surface up the final value of n on the cathode surface. The lengths on the sides of each area are called $d0$, $d1$, $L0$ and $L1$.

Being a 2 dimensional problem J represents the current per unit of perpendicular length, and ρ represents the charge per unit of surface.

The iterative calculation is done between each pair of field lines (see Figure 8) by:

$$\rho_n = J_n/(\mu E_n) \tag{51}$$

where J_n is J at the location of E_n, and it is known for a given K, and

$$E_{n+1} = (\rho_n d_{av} L_{av}/\epsilon_0 + d0\ E_n)/d1 \tag{52}$$

where $d_{av} = (d0+d1)/2$ and $L_{av} = (L0+L1)/2$. Those are the numerical implementations of (2) and (3).

The initial condition for the iteration is Kaptzov assumption[23] (explained in the introduction), which requires:

$$E_0 = E_i \tag{53}$$

After finishing the calculation between the first two field lines (i.e. in the region of very small y we check the result of $\int_a^b E\,\mathrm{d}x \approx \sum_n E_n L_{av_n}$. Say its value is $2V_0$, we have to reduce K by a factor of approximately 4 (approximate because the initial condition for E is independent on K). This process converges very quickly (3-4 iterations), and after establishing K we can process the calculations.

As explained in Sect. 3, as we get farther from the straight fields lines region, the errors slowly increase, getting bigger and bigger when approaching the Warburg[19,20] limit region (see Figure 7).

This is correctable by letting K decrease with v (this way $\bar{\nabla} \cdot \bar{J}$ remains 0, as it should). We implemented a fixed K within the Warburg region, letting it drop to 0 outside the region, although a smooth change may have been considered too.

It is to mentioned that this correction is also in accordance with the experimental knowledge that the current drops to 0 outside the Warburg region[27–30].

Within each area element we also calculate the x component of the force

$$F_{x_n} = E_{x_n} \rho_n \tag{54}$$

where E_{x_n} is the x component of E_n. The total force is eventually summed on the whole area, and knowing J we sum across the line fields (in the v direction), obtaining the total current I.

In the final stage the force and the current are multiplied by 2 to account for the symmetric $y < 0$ region and the values being per unit of length of the lifter, are multiplied by the perimeter $0.6m$. The force is normalized to show the lifted mass in grams.

The values of V_0 for which we did the calculations, have been chosen to fit the values on which the experiment has been done (see next section).

The calculated results are presented in Table I

TABLE I: Calculated results

V_0 $[Kv]$	Current [mA]	Mass that can be lifted [g]
11.12	0.084	1.54
12.9	0.145	2.65
14.08	0.19	3.55
14.4	0.219	4
15.64	0.27	4.98
16.8	0.34	6.16
18.9	0.46	8.42
20.5	0.586	10.74
21.8	0.678	12.44
22.8	0.76	13.9

6. THE EXPERIMENT

The experiment is shown in Figure 9.

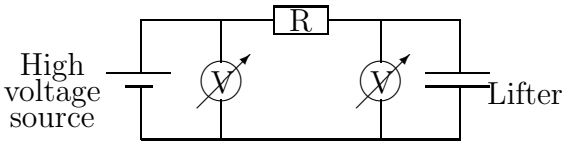

FIG. 9: The configuration of the experiment. The lifter is connected to a high voltage source through a resistor. For different values of resistors, the input and lifter voltages are measured.

For different values of resistors, the input and lifter voltages are measured and the lifting force is measured. The lifting force has been measured only for the cases for which the lifter lifted, by counter balancing it, knowing that its mass is $7g$.

The results of the measurements are shown Table II. The current is calculated using the 2 measured voltages and the resistor.

7. COMPARISON AND APPROXIMATED FORMULAE

TABLE II: Measured results (NA means not available)

R [$M\Omega$]	Lifter voltage V_0 [Kv]	Source voltage [Kv]	Current [mA]	Lifted mass [g]
308	11.12	25.6	0.047	NA
154	12.9	25.58	0.082	NA
110	14.08	25.51	0.104	NA
88	14.4	25.46	0.126	NA
66	15.64	25.42	0.148	NA
44	16.8	25.3	0.193	NA
22	18.9	25	0.277	7.5
10	20.5	25	0.450	10
6.8	21.8	24.92	0.459	12.2
3.3	22.8	24.8	0.606	13

One may see that the calculated forces fit well to the measured force. We will now analyze the current-voltage relation for the calculated and measured results. Those are shown in Figure 10.

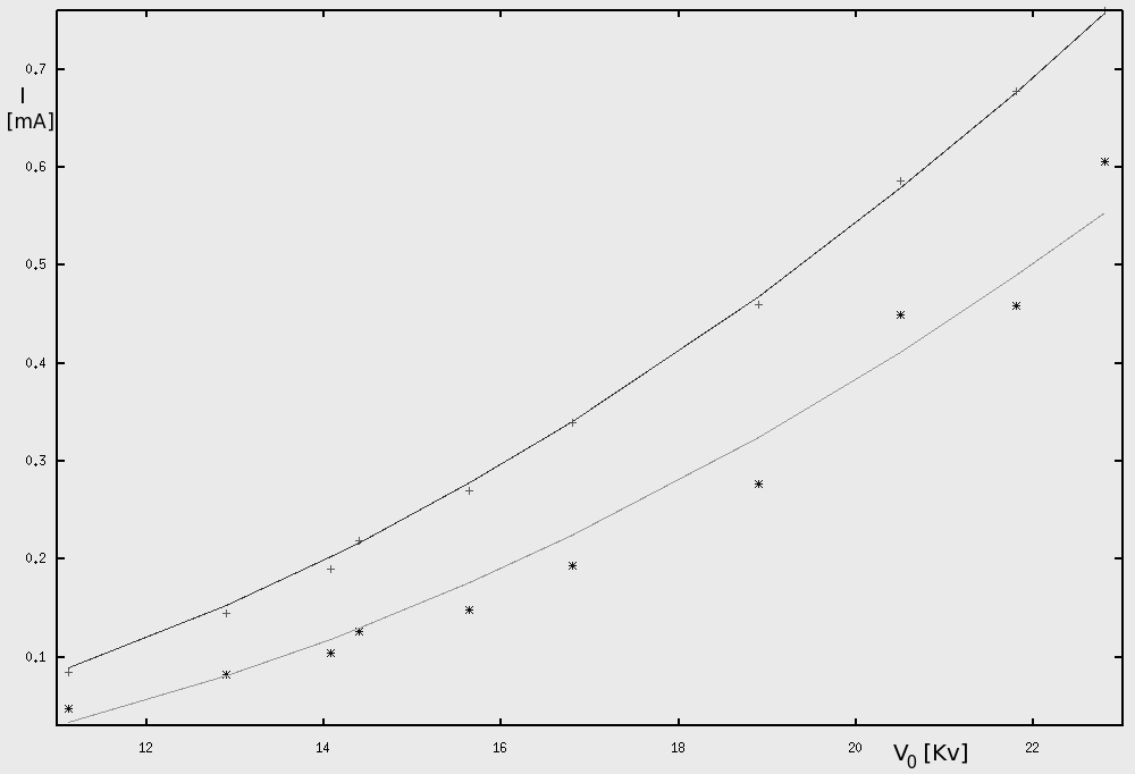

FIG. 10: The current-voltage curve of the lifter. The '*' describe the measured results and the '+' describe the calculated results. The continuous curves are the closest approximations to the above results using $I = K_1 V_0 (V_0 - \mathrm{CIV})$

We remark that both measured and calculated results may be curve fitted with Townsent[26] formula:

$$I = K_1 V_0 (V_0 - \mathrm{CIV}) \tag{55}$$

although the measured results look farther from their fitted curve than the calculated results (might be because of some technical problems during experiment).

The curve fitted to the calculated results used $K_1 = 21.6 \times 10^{-4} mA/(Kv)^2$ and CIV = 7.42Kv, while this fitted to the measured results used $K_1 = 18.2 \times 10^{-4} mA/(Kv)^2$ and CIV = 9.46Kv.

The constant[26] is known to be proportional to the ion mobility μ and to the capacitance, and inverse proportional to the square distance between the electrodes b^2. Checking for the proportionality factor (after putting everything in MKS units) we find that:

$$K_1 = 1.9 \mu C / b^2 \tag{56}$$

and here one may see that the differences between the measured and calculated K_1 fit the differences between the measured and calculated capacitances.

The fact that the measured and calculated force resemble, and we see from Table I that the force is proportional to the current, i.e. mass divided by current is 18.34 g/mA, we may write the relation between force and current:

$$\frac{F}{I} = 179.72 N/A \tag{57}$$

We know that for a lifter with parallel field lines (like a series of parallel thin anode wires over a platform of parallel vertical cathode surfaces) - see[13], one may derive a very simple relation between force and current: $F = \iiint E\rho \mathrm{dv}$. According to (2) $E\rho = J/\mu$, hence we get for constant μ: $F = (1/\mu) \iiint J \mathrm{dv}$. The integral over the coordinates perpendicular to J (v,z in Figure 7) result in the total current I, hence: $F = (I/\mu) \int \mathrm{du}$, and the last integral is just the distance between the electrodes - let us call it d. So for the parallel field lifter one obtains: $F = (Id/\mu)$.

Expressing the same way (57), we obtain:

$$F = \frac{I(1.284b)}{\mu} \tag{58}$$

The factor 1.284 which multiplies the distance between electrodes b can be understood as a lengthening factor. This means that $1.284b$ can be viewed as the average length of the field lines (see Figure 7).

Hence we obtained an approximate formula (58) for calculating the force of a lifter build as a thin anode over a vertical cathode surface. The current I to be set in (58) can be calculated from (55) and (56), and the CIV can be calculated from (49) and (48).

CONCLUSIONS

In this paper we calculated to force on a levitation unit, built as a thin anode wire over a vertical cathode plane, as the electric force on the space charge and compared with experiment.

Our calculations were based on the Laplacian solution for this electrostatic configuration, which by itself is a new result.

With the aid of the Laplacian solution, Deutsch assumption and a first order correction we were able to calculate the force on the levitation unit and the current. The calculated results showed a good correspondence with the measured results.

Also, based on the known formula which describes the force as the current multiplied by the distance between electrodes (when this distance is constant) and divided by the ion mobility, we interpreted our result as basically describing the force in the way mentioned above, with the distance taken as $1.284b$, which may be understood as the average length of the field lines.

---

* Electronic address: riancon@mail.shenkar.ac.il

[1] T.T. Brown, "A method of and an apparatus or machine for producing force or motion" , British Patent 300311, (1928)

[2] T.T. Brown, "Electrostatic motor", US Patent 1974483, (1934)

[3] T.T. Brown, "Electrokinetic Apparatus", US Patent 2949550, (1960)

[4] Website dedicated to BB effect "http://www.biefeldbrown.com/"

[5] Jean-Louis Naudin website "http://jnaudin.free.fr/"

[6] Tajmar M. and de Matos, C.J.,"Coupling of electromagnetism and gravitation in the weak field approximation", *Journal of Theoretics*, **Vol.3** (1), (Feb/March 2001).

[7] Musha T., "Theoretical explanation of the Biefeld-Brown Effect", *Electric Space Craft Journal*, **Issue 31** (2000).

[8] Website "http://montalk.net/science/84/the-biefeld-brown-effect"

[9] T.B. Bahder, C. Fazi, "Force on an asymmetrical capacitor, *Army Research Laboratory*, Report No. ARL-TR-3005, (March 2003)

[10] Tajmar M. "Biefeld-Brown Effect: Misinterpretation of Corona Wind Phenomena", *AIAA Journal*, **Vol.42** (2), 315-318 (2004).

[11] L. Zhao, K. Adamiak, "EHD gas flow in electrostatic levitation unit", *Journal of Electrostatics*, **Vol. 64**, 639-645 (July 2006)

[12] L. Zhao, K. Adamiak, "Numerical analysis of forces in an electrostatic levitation unit", *Journal of Electrostatics*, **Vol. 63**, 729-734 (June 2005)

[13] Website "http://www.blazelabs.com/"

[14] W. Deutsch, "Uber die Dichteverteilung unipolarer Ionenstrome", *Annalen der Physik*, **Vol. 16**, 588-612 (1933)

[15] L. E. Tsyrlin *Sov. Phys.-Tech. Phys.* **Vol. 30** (1958)

[16] A. Ieta, Z. Kucerovsky and W. D. Greason, "Laplacian approximation of Warburg distribution" *Journal of Electrostatics*, **Vol. 63 (2)**, 143-154 (February 2005)

[17] R.S. Sigmond, "Simple approximate treatment of unipolar space-charge-dominated coronas: the Warburg law and the saturation current", *J. Appl. Phys.*, **Vol. 53 (2)**, 891-898 (1982)

[18] J. E. Jones and M. Davies, "A critique of the Deutsch assumption", *J. Phys. D: Appl. Phys.*,

Vol. 25 (12), 1749-1759 (1992)

[19] E. Warburg, "Uber die spitzenentladung", *Wied. Ann* 67-69 (1899).

[20] E. Warburg, "Characteristik des spitzenstromes", *Handbuch der Physik (Springer, Berlin)*, **Vol. 14**, 154-155 (1927).

[21] F.W. Peek "Dielectric Phenomena in High Voltage Engineering", **McGraw-Hill** (1929)

[22] M. Davies, A. Goldman, M. Goldman and J.S. Jones "Developments in the theory of corona corrosion for negative coronas in air", *Proc. XVIII Int. Conf. on Phenomena in Ionized Gases (ICPIG)*, (1987)

[23] N. Kaptzov, "Elektricheskie Yavlenia v Gazakh I Vakuumme", **Ogiz, Moscow**, 587-630 (1947)

[24] N.J. Felici, "Recent advances in the analysis of D.C. ionized electric fields", **Direct Current**, **Vol. 8 (10)**, 278-287 (1963)

[25] J.Q. Feng, "An analysis of corona currents between two concentric cylindrical electrodes", *Journal of Electrostatics*, **Vol. 46**, 37-48 (1998)

[26] J. S. Townsend, *Philos. Mag.*, **Vol. 28**, p83 (1914).

[27] Y. Kondo and Y. Miyoshi, *Jpn. J. Appl. Phys.*, **Vol. 17**, 643 (1978).

[28] A. Goldman, E. O. Selim, and R. T. Waters, *The 5th International Conference on Gas Discharges, lEE Conf. Publ.*, **No. 165** pp. 88-91, (London, 1978).

[29] E. O. Selim and R. T. Waters, *Proceedings of the 3rd International Symposium on High Voltage Engineering*, Paper 53.03, (Milan, 1979)

[30] E. O. Selim and R. T. Waters, *The 6th International Conference on Gas Discharges and their Applications, lEE Conf. Publ.*, **No. 189**, pp. 146-149, (London, 1980)